

# Simulating the Evacuation Process Involving Multitype Disabled Pedestrians

Wenhan Wu<sup>1</sup>, Wenfeng Yi, Jinghai Li, Maoyin Chen<sup>2</sup>, *Member, IEEE*, and Xiaoping Zheng<sup>3</sup>

**Abstract**—The study of crowd evacuation has received considerable attention as the frequent occurrence of crowd disasters in public places. Notably, the increasing proportion of disabled pedestrians makes vulnerable crowds an indispensable part of the evacuation process. However, most previous research neglects to introduce the motion characteristics of disabled pedestrians into the modeling of crowd evacuation. Therefore, we develop an extended model to simulate the evacuation process involving nondisabled, visual-disabled, acoustic-disabled, and physical-disabled pedestrians. Numerical simulations indicate that this model achieves a more realistic mixed crowd evacuation in the library scene and reproduces the escape movement of multitype disabled pedestrians. Moreover, several management strategies are provided to guide the evacuation of disabled pedestrians, and the appropriate strategy can be determined by comprehensively considering multiple factors such as efficiency, safety, and cost.

**Index Terms**—Collective motion, crowd evacuation, disabled pedestrians, management strategy, nonlinear system.

## I. INTRODUCTION

OWING to the increasing frequency of crowd disasters around the world [1], such as the Hajj stampede in Saudi Arabia (in 2006, 634 casualties) [2] and the Love Parade disaster in Germany (in 2006, more than 500 casualties) [3], crowd evacuation has become a critical subject within the field of safety science [4]. With the development of auxiliary devices and humanized facilities, the proportion of disabled pedestrians in public places is universally growing [5]. However, only a few studies have endeavored to consider the impact of disabled pedestrians on crowd evacuation [6], [7]. More critically, there are obvious differences in behavioral characteristics among multitype disabled pedestrians, which poses a huge challenge to crowd evacuation management in emergency situations [8]. As a result, establishing a crowd motion model involving multitype disabled pedestrians is essential for evacuation planning [9].

Manuscript received 17 February 2022; revised 29 April 2022 and 11 June 2022; accepted 10 July 2022. Date of publication 20 July 2022; date of current version 2 October 2023. This work was supported in part by the National Key Research and Development Program of China under Grant 2020YFF0304900, in part by the National Major Scientific Research Instrument Development Project under Grant 61927804, and in part by the National Natural Science Foundation of China under Grant 61773233. (*Corresponding author: Xiaoping Zheng.*)

Wenhan Wu, Wenfeng Yi, Maoyin Chen, and Xiaoping Zheng are with the Department of Automation, Beijing National Research Center for Information Science and Technology, Tsinghua University, Beijing 100084, China (e-mail: wwh19@mails.tsinghua.edu.cn; ywf19@mails.tsinghua.edu.cn; mychen@mail.tsinghua.edu.cn; asean@mail.tsinghua.edu.cn).

Jinghai Li is with the School of Mechanical and Electrical Engineering, Beijing University of Chemical Technology, Beijing 100029, China (e-mail: ljhai725@163.com).

Digital Object Identifier 10.1109/TCSS.2022.3190685

It is well known that relevant dynamics models for crowd evacuation have been mainly divided into macroscopic and microscopic aspects [10]. Macroscopic models are capable of revealing a lot of intriguing phenomena from a whole viewpoint [11], however, those factors involving local interaction with individuals and environments are neglected. Given that the behavioral characteristics of disabled pedestrians are generally reflected at the individual level, we concentrate more on microscopic models such as the cellular automata model [12], agent-based model [13], and social force model [14], [15]. These typical models treat the crowd as a multiagent system, with explicit rules or differential equations updating the velocity and position of each pedestrian [16]. Even though it is flexible and convenient to incorporate individual features into microscopic models, vulnerable crowds such as people with disabilities are rarely taken into account.

To our knowledge, several previous studies have attempted to improve microscopic models to replicate the movement patterns of disabled pedestrians. With regard to cellular automata models, Kim *et al.* [17] proposed a novel model combining the physical characteristics of handicapped pedestrians to explore the impact on traffic flow, whereas other types of disabled pedestrians other than those with physical impairments were neglected. Regarding agent-based models, Christensen and Sasaki [18] constructed an agent-based BUMMPEE model to represent the diversity of disabled pedestrians, which were independently defined by variations in speed, size, and ability to negotiate the terrain. Koo *et al.* [19], [20] further enhanced the BUMMPEE model in terms of time advance mechanism to study the effect of disabled pedestrians on crowd evacuation and formulated evacuation strategies in a high-rise building to improve safety and efficiency. Nevertheless, the above models are mainly implemented by program modules and lack explicit mathematical expressions, which makes the application process complicated. In terms of social force models, Stuart *et al.* [21] provided a hybrid model based on the social force model and fractional order potential fields to describe diverse disabled pedestrians. However, only the desired speed is used to describe the difference between various types of crowds, and heterogeneous features of disabled pedestrians are not fundamentally integrated into this model. As a result, it is expected to find a better model to describe the evacuation process involving multitype disabled pedestrians.

In this article, we develop an extended model to simulate the mixed crowd evacuation of multitype pedestrians. The feature parameters and relevant expressions are incorporated into the behavioral heterogeneity-based social force model

(BHSFM) [22], [23] to reflect the movement characteristics of disabled pedestrians. The equations of motion are employed to quantify the escape movement of nondisabled, visual-disabled, acoustic-disabled, and physical-disabled pedestrians. This model produces a more realistic mixed crowd evacuation by performing numerical simulations in a library scene. The corresponding phenomena show that multitype disabled pedestrians require more attention since they are in a vulnerable situation when attempting to escape. In addition, three management strategies are offered to help disabled pedestrians evacuate more efficiently, and a more appropriate management strategy may be chosen after evaluating different influencing elements. These findings of this study have significant implications for guiding the mixed crowd evacuation involving multitype disabled pedestrians.

The rest of this article is organized as follows. Section II proposes the equations of motion for multitype pedestrians. In Section III, numerical simulations are conducted in a library scene. Section IV elaborates on the corresponding conclusions and further discussions.

## II. MODEL

In recent years, many existing theories and models in evacuation dynamics have been proposed, including social identity theory [24], leader–follower principle [25], discrete models (e.g., cellular automata model [12], lattice gas model [26]), continuous models (e.g., nomadic model [27], social force model [14], [15]), and so on. These approaches are further developed into service mechanisms and simulator systems (e.g., ESCAPE [28], EPES [29]) to solve evacuation planning problems more effectively. The social force model based on Newtonian mechanics is highly flexible, extensible, and fine-grained and reproduces a series of self-organization phenomena such as lane formation, herding effect, and fast-is-slow effect [30]. Therefore, this model is selected for improvement to simulate the evacuation process of multitype pedestrians, which is also beneficial for subsequent embedding in simulation frameworks and application software.

### A. Nondisabled Pedestrians

In light of the heterogeneous characteristics of pedestrians at the behavioral level, we adopt the previously published model [23] to simulate the escape movement of nondisabled pedestrians during evacuation.

1) *Behavioral Heterogeneity Coefficient*: The behavioral heterogeneity coefficient of pedestrian  $i$  is expressed by

$$H_i(t) = \exp(\lambda)\{[1 - p_i(t)]\theta_i P_i(t) + p_i(t)P_i(t)\} \times [(1 - \Delta_M) + 2\Delta_M \psi_i(t)]. \quad (1)$$

One aspect is the physique coefficient  $P_i(t)$  that reflects the high stability physiology attributes, accompanied by 1-D Brownian motion in emergency situations

$$P_i(t + \Delta t) - P_i(t) \sim \mathcal{N}(0, \lambda^2 \Delta t) \quad (2)$$

where  $\Delta t$  is the time step,  $\mathcal{N}(\cdot)$  indicates the normal distribution, and the risk index  $\lambda \in [0, 1]$  is used to measure

the degree of emergency. The fluctuation interval of  $P_i(t)$  is limited to  $[(1 - \Delta_P)P_i(t_0), (1 + \Delta_P)P_i(t_0)]$ , where  $\Delta_P$  represents the maximum fluctuation range, and  $P_i(t_0) = \mu + \sigma X_i$  is the initial physique coefficient, in which a random variable  $X_i \sim \text{Beta}(\alpha, \beta)$ , the location-scale parameters  $\mu$  and  $\sigma$  determine the lower bound and the interval range, respectively.

The other terms in (1) are related to psychology attributes. Here, a ratio factor  $\theta_i$  is defined as the desired speed in normal divided by the maximum desired speed in panic. The panic parameter  $p_i(t)$  is used to describe the impatience degree. The mental state of pedestrian  $i$  can be transformed into cooperation or competition through the state transition function  $\psi_i(t)$  with the maximum mutation  $\Delta_M$

$$\psi_i(t) = \frac{1}{1 + \exp[-\eta_i \rho_i(t) k_M]} \quad (3)$$

where  $k_M$  indicates its slope,  $\rho_i(t) = n_i(t)/\pi \tilde{r}_i^2$  is the pedestrian density in a circular personal zone with radius  $\tilde{r}_i \approx 4r_i$ , and  $n_i(t)$  is the number of pedestrians in this zone. The state selection variable  $\eta_i = -1$  with cooperation probability  $\gamma_i(\lambda)$ , while  $\eta_i = +1$  if it falls in competition probability  $1 - \gamma_i(\lambda)$ . Here,  $\gamma_i(\lambda) = \gamma_0 \exp(-w_i \lambda)$ , where  $\gamma_0$  is the normal cooperation probability in nonemergency situations, and  $w_i$  denotes the attenuation rate.

2) *Equations of Motion for Nondisabled Pedestrians*: The BHSFM describes the movement of nondisabled pedestrians, which is performed by the following equations of motion:

$$m_i \frac{d\mathbf{v}_i(t)}{dt} = m_i \frac{H_i(t)v_i^0 \mathbf{e}_i^0 - \mathbf{v}_i(t)}{\tau_i} + \sum_{j(\neq i)} \mathbf{f}_{ij} + \sum_W \mathbf{f}_{iW}. \quad (4)$$

The first term of the right formula reflects the self-driven force affected by behavioral heterogeneity coefficient  $H_i(t)$ . Here, pedestrian  $i$  of mass  $m_i$  and radius  $r_i$  tends to escape with a desired speed  $H_i(t)v_i^0$  in a desired direction  $\mathbf{e}_i^0$ , and adapts the actual velocity  $\mathbf{v}_i(t)$  within a relaxation time  $\tau_i$ .

The second term  $\mathbf{f}_{ij}$  illustrates the interaction force between pedestrian  $i$  and  $j$

$$\mathbf{f}_{ij} = A_i \exp[(r_{ij} - d_{ij})/B_i] \mathbf{n}_{ij} + kg(r_{ij} - d_{ij}) \mathbf{n}_{ij} + \kappa g(r_{ij} - d_{ij}) \Delta v_{ji}^t \mathbf{t}_{ij} \quad (5)$$

where  $A_i$  and  $B_i$  are constants,  $r_{ij}$  is the radius sum of pedestrian  $i$  and  $j$ ,  $d_{ij}$  is the distance between the centroids of them, and  $\mathbf{n}_{ij}$  denotes the normalized vector from pedestrian  $j$  to  $i$ .  $k$  and  $\kappa$  determine the obstruction effects in physical interactions,  $\Delta v_{ji}^t$  is the tangential velocity difference, and  $\mathbf{t}_{ij}$  represents the tangential direction. Besides,  $g(x)$  is zero if  $x > 0$ , and otherwise it equals to  $x$ .

The last term  $\mathbf{f}_{iW}$  is created analogously by the interaction between pedestrian  $i$  and the walls

$$\mathbf{f}_{iW} = A_i \exp[(r_i - d_{iW})/B_i] \mathbf{n}_{iW} + kg(r_i - d_{iW}) \mathbf{n}_{iW} - \kappa g(r_i - d_{iW})(\mathbf{v}_i \cdot \mathbf{t}_{iW}) \mathbf{t}_{iW}. \quad (6)$$

Here,  $d_{iW}$  is the distance to the wall  $W$ , and  $\mathbf{n}_{iW}$  and  $\mathbf{t}_{iW}$  represent the normalized vector perpendicular and the tangential direction to it, respectively. Note that other terms are consistent with that in the second term.

### B. Disabled Pedestrians

The disabled pedestrians often lack the capacity to evacuate autonomously, because visual and acoustic impairments limit the perception of emergency, and physical impairments make it difficult for pedestrians to move flexibly [31]. In this section, the escape movements of visual-disabled, acoustic-disabled, and physical-disabled pedestrians are modeled by different equations of motion.

#### 1) Equations of Motion for Visual-Disabled Pedestrians:

The behavioral heterogeneity coefficient  $H_i^{\text{vis}}(t)$  of visual-disabled pedestrians differs from that of nondisabled pedestrians, which is mainly reflected in assigning values. In terms of physiology attributes, physical escape behaviors are weakened by visual impairments to a certain extent, the distribution curve is thereby adjusted to produce overall weaker physiology characteristics by altering the shape parameters in Beta distribution. Turning to psychology attributes, the maximum mutation  $\Delta_M$  is cleared to ignore the transition of mental state as visual-disabled pedestrians cannot perceive their surrounding individuals using visual information. Thereby, the extended social force model for visual-disabled pedestrians is given by

$$m_i \frac{d\mathbf{v}_i(t)}{dt} = m_i \frac{H_i^{\text{vis}}(t)v_i^0 \mathbf{e}_i^{\text{vis}}(t) - \mathbf{v}_i(t)}{\tau_i} + \sum_{j(\neq i)} \mathbf{f}_{ij} + \sum_W \mathbf{f}_{iW}. \quad (7)$$

Because it is hard for pedestrian  $i$  to effectively obtain evacuation information through vision, the desired direction  $\mathbf{e}_i^{\text{vis}}(t)$  is defined as the weighted sum of initial desired direction  $\mathbf{e}_i^0$  and random disturbance direction  $\varepsilon_i(t)$

$$\mathbf{e}_i^{\text{vis}}(t) = \frac{\varpi_i^{\text{vis}} \varepsilon_i(t) + (1 - \varpi_i^{\text{vis}}) \mathbf{e}_i^0}{\|\varpi_i^{\text{vis}} \varepsilon_i(t) + (1 - \varpi_i^{\text{vis}}) \mathbf{e}_i^0\|} \quad (8)$$

where  $x$  and  $y$  coordinates of  $\varepsilon_i(t)$  are independent Gaussian noises, which are time-correlated but independent for different individuals,  $\langle \varepsilon_i(t) \varepsilon_j(s) \rangle = \delta_{ij} \delta(t-s)$ . The feature parameter  $\varpi_i^{\text{vis}} \in (0, 1)$  represents the influence degree of random disturbance direction, depending on those factors such as the familiarity with scenes and the information acquired from other senses. Given that visual-disabled pedestrians are difficult to observe their surroundings, the second term  $\mathbf{f}_{ij}$  and the last term  $\mathbf{f}_{iW}$  ignore psychological repulsive forces with other individuals and the walls.

#### 2) Equations of Motion for Acoustic-Disabled Pedestrians:

The biggest obstacle restricting acoustic-disabled pedestrians is the inability to perceive sound signals (e.g., alarms, explosions, and shouts), especially when the danger source is outside the scenario. The evacuation process of acoustic disabled pedestrians can be divided into two stages. First, before pedestrian  $i$  is aware of the danger, he/she will maintain the previous behavior (stay at the original place). Second, pedestrian  $i$  will escape like other nondisabled pedestrians after he/she realizes the necessity for evacuation. In this case, the duration is defined as  $t_i^{\text{aco}}$  before the escape consciousness of pedestrian  $i$  is activated. The extended social force model

for acoustic-disabled pedestrians is given by

$$m_i \frac{d\mathbf{v}_i(t)}{dt} = m_i \frac{H_i^{\text{aco}}(t)v_i^0 \mathbf{e}_i^0 - \mathbf{v}_i(t)}{\tau_i} + \sum_{j(\neq i)} \mathbf{f}_{ij} + \sum_W \mathbf{f}_{iW}. \quad (9)$$

Here, the behavioral heterogeneity coefficient  $H_i^{\text{aco}}(t)$  is zero if  $t < t_i^{\text{aco}}$ , otherwise its parameters and values are consistent with that of nondisabled pedestrians. It is assumed that  $t_i^{\text{aco}}$  depends on the first time when pedestrian  $i$  perceives that the local speed at its position  $\mathbf{x}_i$  exceeds a sensitive threshold, which satisfies the mathematical form as  $t_i^{\text{aco}} = \min\{t | v(\mathbf{x}_i, t) \geq \varpi_i^{\text{aco}} \text{ m} \cdot \text{s}^{-1}\}$ . Here, the sensitive threshold is denoted by the feature parameter  $\varpi_i^{\text{aco}} > 0$ , and the local speed is calculated as follows:

$$v(\mathbf{x}_i, t) = \frac{\sum_j \|\mathbf{v}_j\| f(\mathbf{x}_j(t) - \mathbf{x}_i)}{\sum_j f(\mathbf{x}_j(t) - \mathbf{x}_i)} \quad (10)$$

where  $\mathbf{x}_j(t)$  are the positions of other pedestrians  $j$  at time  $t$ , and  $f(\mathbf{x}_j(t) - \mathbf{x}_i)$  represents a Gaussian distance-dependent weight function

$$f(\mathbf{x}_j(t) - \mathbf{x}_i) = \frac{1}{\pi R^2} \exp\left[-\|\mathbf{x}_j(t) - \mathbf{x}_i\|^2 / R^2\right] \quad (11)$$

where  $R$  is a measurement parameter, the value of which is equal to radius  $\tilde{r}_i$  in a personal zone. The interaction forces  $\mathbf{f}_{ij}$  and  $\mathbf{f}_{iW}$  are the same as that in the social force model, because acoustic-disabled pedestrians can normally interact with other individuals and the walls.

3) *Equations of Motion for Physical-Disabled Pedestrians:* The behavioral heterogeneity coefficient of physical-disabled pedestrians  $H_i^{\text{phy}}(t)$  also exists obvious differences. As this kind of pedestrians generally use auxiliary mobile tools (e.g., crutches, wheelchairs, etc.) to evacuate, the scale parameter is adjusted to reduce the interval of physique coefficient, in accord with the movement inconvenience. Given that physical-disabled pedestrians are frequently blocked due to high space occupancy and limited mobility, their psychological competitiveness may be stronger by increased impatience [15], we therefore enhance the cooperation attenuation rate  $w_i$  to tally with it. Based on the above adjustments, the extended social force model for physical-disabled pedestrians is given by

$$m_i \frac{d\mathbf{v}_i(t)}{dt} = m_i \frac{H_i^{\text{phy}}(t)v_i^0 \mathbf{e}_i^0 - \mathbf{v}_i(t)}{\tau_i^{\text{phy}}} + \sum_{j(\neq i)} \mathbf{f}_{ij} + \sum_W \mathbf{f}_{iW}. \quad (12)$$

Here, the acceleration process from adapting the actual speed to the desired speed is relatively longer since the autonomous movement is restricted, the relaxation time  $\tau_i^{\text{phy}}$  of pedestrian  $i$  is therefore obtained as follows:

$$\tau_i^{\text{phy}} = \varpi_i^{\text{phy}} \tau_i \quad (13)$$

where  $\varpi_i^{\text{phy}} > 1$  is the feature parameter denoting the delay degree of relaxation time, and a larger  $\varpi_i^{\text{phy}}$  indicates a higher delay degree caused by auxiliary mobility tools. Moreover, the interaction forces  $\mathbf{f}_{ij}$  and  $\mathbf{f}_{iW}$  are the same as that in the social force model except for the radius of physical-disabled



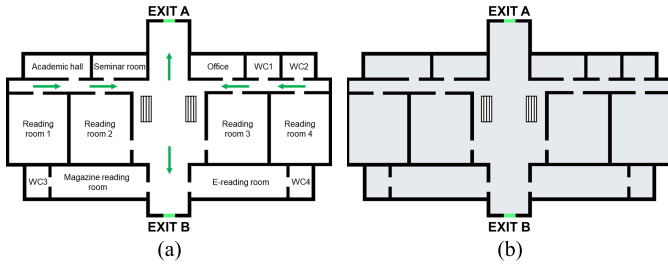


Fig. 1. Schematic diagram of the simulation scene. (a) 2-D floor plan of the library scene. (b) Pedestrian spawning areas in the 2-D floor plan (in gray). The global size of the real scenario is 70-m length and 42.5-m width, and each pixel of the library scene is equal to a square with a 0.1-m side.

pedestrians, which is expanded as  $r_i^{\text{phy}} = r_i + \Delta l$  to highlight the larger space occupied by auxiliary mobile tools.

### III. NUMERICAL SIMULATIONS

#### A. Simulation Setup

Compared with able-bodied people, people with disabilities are less likely to pursue higher education and obtain meaningful employment [32]. In light of the limited mobility, they are more likely to engage in daily activities that reduce or avoid movements. Consequently, the governments have established some public institutions serving the disabled to reflect humanistic concerns. One of the typical institutions is the library, part of which is advocated to design for the disabled or provide disabled service areas [33]. In this case, the numerical simulations are conducted in a library scene, in which some important areas are preserved, while other irrelevant areas are abandoned. Besides, a hypothesis for simplicity is stressed that those disabled pedestrians accompanied by their nondisabled peers are not included in our simulations, even though this phenomenon exists in actual situations.

Fig. 1(a) shows the 2-D floor plan of the library scene, the global size of which is 70-m length and 42.5-m width. The library has an academic hall (15 m  $\times$  5.5 m), a seminar room (12 m  $\times$  5.5 m), an E-reading room (21 m  $\times$  7.5 m), a magazine reading room (21 m  $\times$  7.5 m), an office (12 m  $\times$  5.5 m), four reading rooms (13.5 m  $\times$  15.5 m), and four WCs (7.5 m  $\times$  5.5 m). The black bars represent the walls, and two green strip areas correspond to EXIT A and EXIT B with 2.5-m width. Fig. 1(b) depicts that the pedestrian spawning areas are marked in gray in the 2-D floor plan. Incidentally, the 2-D floor plan used for simulation is scaled from the real scenario, where each pixel corresponds to a square with a 0.1-m side.

It is necessary to clarify the parameter settings before conducting numerical simulations. Assuming that the risk index is a constant  $\lambda = 0.5$ , which creates a moderate emergency environment. The number of pedestrians is fixed as  $N = 400$  in the scene, where pedestrians are randomly distributed at the initial time and update their positions and velocities with a time step  $\Delta t = 0.04$  s. Regarding the equations of motion for nondisabled pedestrians, in accord with relevant [15], [23], the setting of parameters and values are summarized in Table I. The parameters and corresponding

TABLE I  
SETTING OF PARAMETERS AND VALUES FOR NONDISABLED PEDESTRIANS

Symbol	Description	Value
$\Delta_P$	Maximum fluctuation range	0.1
$\alpha$	Shape parameter 1	4
$\beta$	Shape parameter 2	4
$\mu$	Location parameter	0
$\sigma$	Scale parameter	3
$k_M$	Mutation slope	0.1
$\Delta_M$	Maximum mutation	0.5
$\gamma_0$	Normal cooperation probability	0.95
$w_i$	Attenuation rate	1.25
$\theta_i$	Ratio factor	0.5
$m_i$	Pedestrian mass	80 kg
$r_i$	Pedestrian radius	0.25 $\sim$ 0.35 m
$v_i^0$	Initial unit speed	1 m s <sup>-1</sup>
$\tau_i$	Relaxation time	0.5 s
$A_i$	Constant 1	2 $\cdot$ 10 <sup>3</sup> N
$B_i$	Constant 2	0.08 m
$k$	Body elasticity coefficient	1.2 $\cdot$ 10 <sup>5</sup> kg s <sup>-2</sup>
$\kappa$	Sliding friction coefficient	2.4 $\cdot$ 10 <sup>5</sup> kg m <sup>-1</sup> s <sup>-1</sup>

values for disabled pedestrians are provided based on the simulation requirements in subsequent contents. Note that only those different from nondisabled pedestrians are indicated, while other parameters remain consistent.

#### B. Evacuation Processes for Different Types of Pedestrians

In this section, the evacuation processes for different types of pedestrians are analyzed separately. According to the investigation of pedestrian speed characteristics [19], relevant parameters are reasonably adjusted for disabled pedestrians as follows:  $\alpha = 2$  for visual-disabled pedestrians, no change for acoustic-disabled pedestrians,  $\sigma = 1.5$ ,  $w_i = 2$ ,  $\Delta l = 0.15$  m for physical-disabled pedestrians, and other parameters are consistent with that of nondisabled pedestrians. To facilitate the numerical simulation, we first assign moderate values to the feature parameters as  $\varpi_i^{\text{vis}} = 0.5$ ,  $\varpi_i^{\text{aco}} = 0.3$ ,  $\varpi_i^{\text{phy}} = 6$  for multitype disabled pedestrians, and later the impact of various feature parameter values on evacuation processes will be discussed in detail.

Fig. 2 displays the snapshots of crowd evacuation involving different types of pedestrians in the library scene. Nondisabled pedestrians are the fastest to escape from the library, visual-disabled pedestrians are relatively slow due to directional interference, partial acoustic-disabled pedestrians escape quickly but other unaware individuals remain, and physical-disabled pedestrians move the slowest and occupy more space. This is an intuitive description of various phenomena in these snapshots, and Fig. 3 further shows the temporal evolution of behavioral heterogeneity coefficients for multitype pedestrians. Compared with other situations, the behavioral heterogeneity coefficients of visual-disabled pedestrians are relatively stable since the dynamic changes in surrounding environments are hard to perceive. The situation of acoustic-disabled pedestrians is noteworthy, because the behavioral heterogeneity coefficients of unaware individuals are zero, implying these pedestrians never leave their original positions. Besides, the behavioral heterogeneity coefficients of physical-disabled



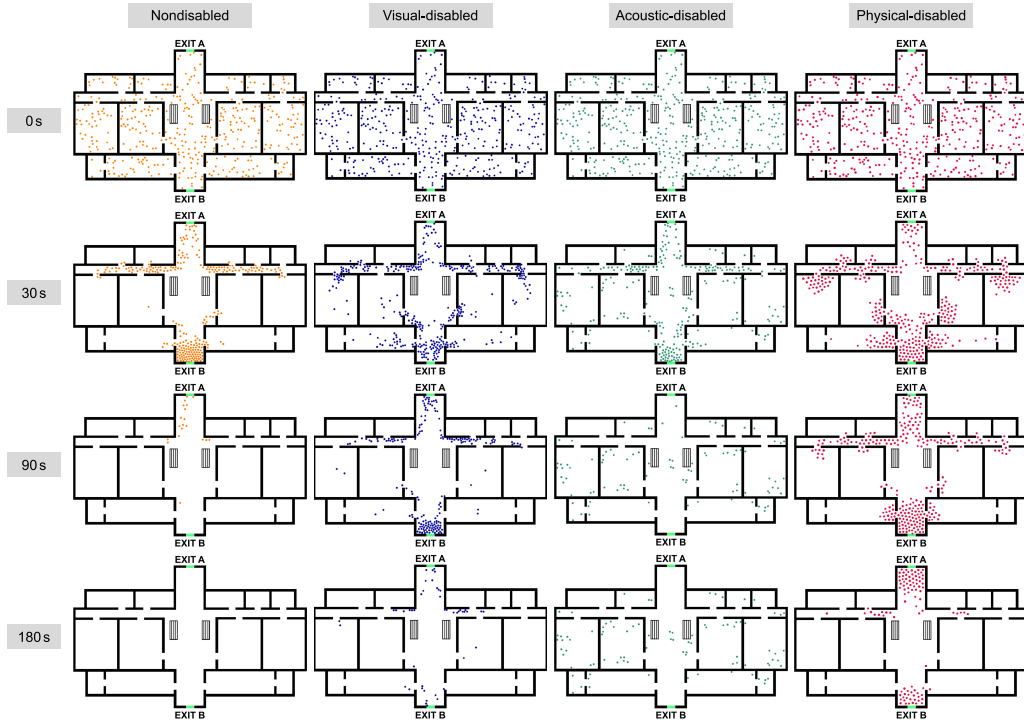


Fig. 2. Snapshots of crowd evacuation involving different types of pedestrians in the library scene. The vertical direction indicates different moments at 0, 30, 90, and 180 s. The horizontal direction denotes different types of pedestrians, where nondisabled, visual-disabled, acoustic-disabled, and physical-disabled pedestrians are represented by orange, blue, green, and pink circles, respectively.

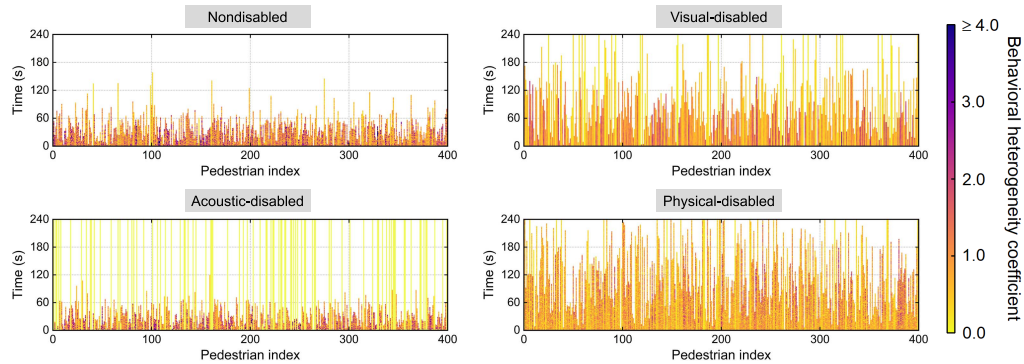


Fig. 3. Temporal evolution of behavioral heterogeneity coefficients for different types of pedestrians. The pedestrian index 0–400 corresponds to each pedestrian spawned on the library scene at the initial time.

pedestrians universally last longer and change repeatedly, which is caused by their mobility impairments and frequent interactions.

The above discussions reveal the evacuation characteristics of different types of pedestrians. It is notable that the feature parameters reflecting the responses to emergencies are also worth examining. Fig. 4 analyzes the evacuation efficiency of disabled pedestrians under various values of feature parameters. Due to the increased impact degree of random disturbance direction, as illustrated in Fig. 4(a), a larger  $\varpi_i^{\text{vis}}$  equates to a slower evacuation efficiency. Acoustic-disabled pedestrians are more likely to perceive evacuation signals when  $\varpi_i^{\text{hea}}$  is smaller, resulting in a faster escape efficiency in Fig. 4(b). Furthermore, as shown in Fig. 4(c), the evacuation efficiency

of physical-disabled pedestrians improves as  $\varpi_i^{\text{phy}}$  increases, this is attributed to the reduction of delay degree caused by auxiliary mobility tools. As a result, the values of feature parameters can be adjusted according to actual conditions to reflect the responses to emergencies of disabled pedestrians.

### C. Quantitative Analysis of Mixed Crowd Evacuation

The crowd in a library designed for the disabled may be made up of multitype pedestrians, and the proportion of disabled pedestrians is much higher than that of ordinary public places. This necessitates us to conduct a detailed analysis of mixed crowd evacuation in the library scene. Given that reading rooms are the primary gathering areas, the crowd in reading rooms is estimated to be 70% of the

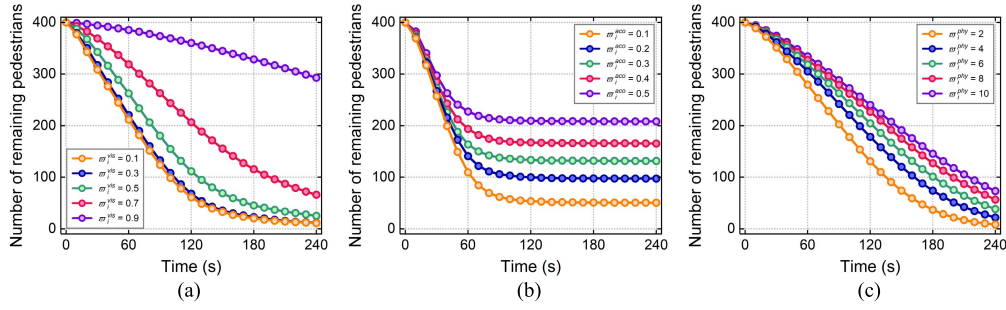


Fig. 4. Number of remaining pedestrians as a function of time under different values of feature parameters. (a) Visual-disabled pedestrians with  $\varpi_i^{\text{vis}} = 0.1, 0.3, 0.5, 0.7, 0.9$ . (b) Acoustic-disabled pedestrians with  $\varpi_i^{\text{aco}} = 0.1, 0.2, 0.3, 0.4, 0.5$ . (c) Physical-disabled pedestrians with  $\varpi_i^{\text{phy}} = 2, 4, 6, 8, 10$ .

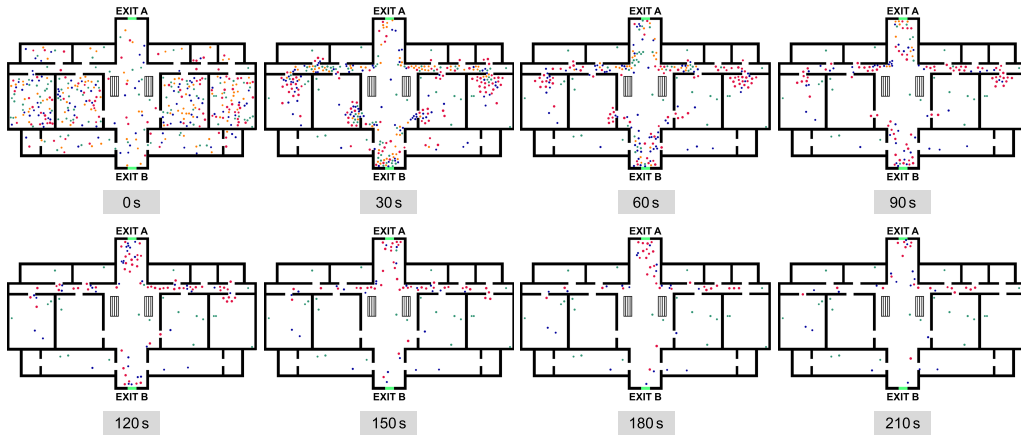


Fig. 5. Snapshots of mixed crowd evacuation in the library scene at 0, 30, 60, 90, 120, 150, 180, and 210 s. The orange, blue, green, and pink circles represent nondisabled, visual-disabled, acoustic-disabled, and physical-disabled pedestrians, respectively.

total, with the remaining 30% distributed in other areas. Due to the variability of responses to emergencies, the feature parameters are regarded as random variables with uniform distributions, where  $\varpi_i^{\text{vis}} \sim U(0.1, 0.9)$ ,  $\varpi_i^{\text{aco}} \sim U(0.1, 0.5)$ , and  $\varpi_i^{\text{phy}} \sim U(2, 10)$ , and other parameters are identical to those settings in Section III-B. The proportions of nondisabled, visual-disabled, acoustic-disabled, and physical-disabled pedestrians are first assumed to be equal, which is beneficial to avoid accidental simulation results and display the evacuation characteristics of multitype pedestrians. Note that the proportions can also be adjusted according to actual situations, and the impact of different proportions of disabled pedestrians on crowd evacuation is accordingly discussed in the subsequent contents.

Fig. 5 performs the snapshots of mixed crowd evacuation in the library scene. Nondisabled and partial acoustic-disabled pedestrians are found to dominate the evacuation process, whereas visual-disabled and physical-disabled pedestrians are mostly at the back of the crowd. To further quantitatively analyze the mixed crowd evacuation, we repeat the simulation 50 times to obtain more reliable results. The probability distributions of average actual speed for different types of pedestrians are depicted in Fig. 6. It is clear that the average actual speed of nondisabled and acoustic-disabled pedestrians shows relatively higher values and larger variations than that of visual-disabled and physical-disabled pedestrians. As shown

in Fig. 7(a), the evacuation efficiency of nondisabled pedestrians is the fastest, and the remaining number is likewise the smallest. The evacuation efficiency of acoustic-disabled, visual-disabled, and physical-disabled pedestrians decreases sequentially in the initial stage, but the situation reverses in the subsequent stage. These findings are collectively reflected in the time-varying proportion of remaining pedestrians in Fig. 7(b), which points out the significance of guiding the evacuation of disabled pedestrians.

The next part is concerned with the impact of an environmental emergency on mixed crowd evacuation. The risk index  $\lambda$  is a critical quantitative indicator used to measure the degree of emergency. As seen in Fig. 8(a), a larger risk index leads to a faster reduction in the number of remaining pedestrians. Apart from the evacuation efficiency, we also focus on the risk of injury caused by pedestrian mutual extrusion. The radial pressure  $\zeta_i(t) = \sum_{j(\neq i)} \|\mathbf{f}_{ij}(t)\| / (2\pi r_i)$  is introduced to measure the degree of body compression [15]. Accordingly, the cumulative radial pressure is defined as the cumulative sum of radial pressure for each pedestrian. In Fig. 8(b), we notice a high risk also expands the cumulative radial pressure, implying a severe emergency may lead to more casualties.

In actual situations, the proportion of disabled pedestrians is diverse, and its impact on mixed crowd evacuation is also worth exploring. Here, we define  $\vartheta$  as the number of the disabled divided by the total number of pedestrians.

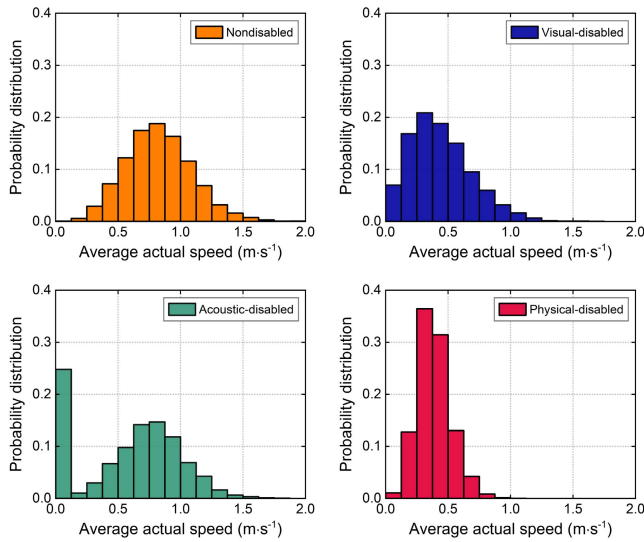


Fig. 6. Probability distributions of average actual speed for different types of pedestrians.

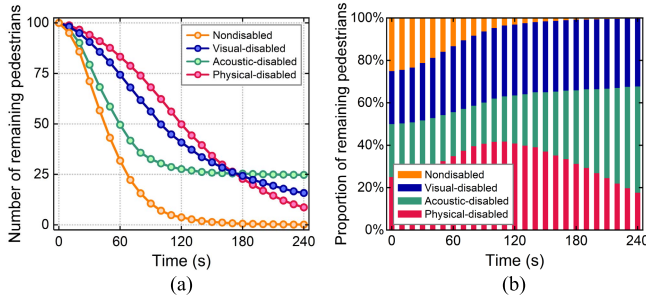


Fig. 7. Analysis of mixed crowd evacuation for different types of pedestrians. (a) Number of remaining pedestrians as a function of time. (b) Time-varying proportion of remaining pedestrians.

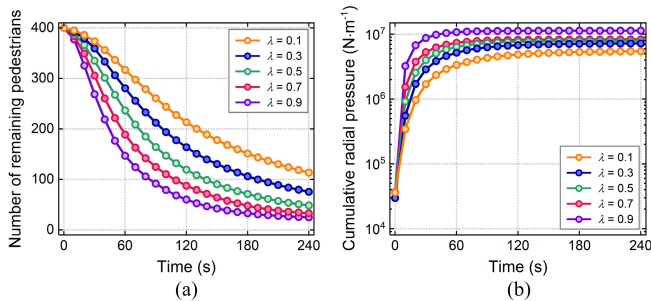


Fig. 8. Analysis of mixed crowd evacuation under different risk indexes. (a) Number of remaining pedestrians as a function of time. (b) Cumulative radial pressure as a function of time.

The proportions are set from low (10%) to high (90%), where the number of each type of disabled pedestrian is fixed to be equal. Fig. 9(a) indicates that the evacuation efficiency gradually decreases as the proportion of disabled pedestrians grows, which is consistent with empirical observations. Meanwhile, as shown in Fig. 9(b), the cumulative radial pressure also increases with the proportion of disabled pedestrians, since the prolonged congestion creates more body collisions. These results imply that a high proportion of disabled pedestrians has multiple negative effects on mixed crowd evacuation.

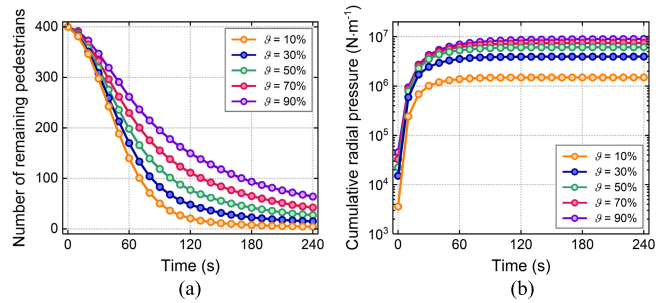


Fig. 9. Analysis of mixed crowd evacuation under different proportions of disabled pedestrians. (a) Number of remaining pedestrians as a function of time. (b) Cumulative radial pressure as a function of time.

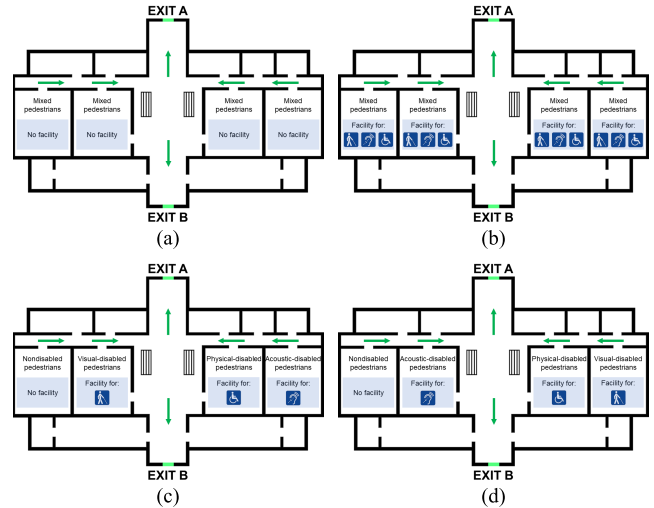


Fig. 10. Schematic diagrams of management strategies for mixed crowd evacuation. (a) Blank group. (b) Strategy 1. (c) Strategy 2. (d) Strategy 3.

#### D. Management Strategies for Mixed Crowd Evacuation

The quantitative analysis of mixed crowd evacuation suggests that different types of disabled pedestrians have various evacuation characteristics, but all belong to vulnerable crowds that necessitate attention. To improve overall evacuation efficiency and reduce casualties of disabled pedestrians, it is vital to offer effective solutions for mixed crowd evacuation. On the one hand, redesigning the structure of buildings (i.e., adjusting the layout, adding specialized exits) is a potential method to increase efficiency and safety [34]. However, it is not adopted here due to the cost of this solution tends to be extremely high. On the other hand, assigning guidance facilities on the scene is also beneficial to assist the evacuation of disabled pedestrians. The optimal effect can be achieved by covering the entire scene with guidance facilities, whereas it will occupy a lot of public space and require a high cost. In this case, guidance facilities for multitype disabled pedestrians are merely considered to be placed in main crowd gathering areas.

Formulating low-cost and reasonable management strategies combined with guidance facilities is critical for optimizing the mixed crowd evacuation process. In the form of schematic diagrams, the blank group without guidance facilities is displayed in Fig. 10(a), and three management strategies are presented in Fig. 10(b)–(d). For Strategy 1,





Fig. 11. Snapshots of mixed crowd evacuation in the library scene under different management strategies. The vertical direction indicates different moments at 0, 30, 90, and 180 s. The horizontal direction denotes different management strategies. The orange, blue, green, and pink circles represent nondisabled, visual-disabled, acoustic-disabled, and physical-disabled pedestrians, respectively.

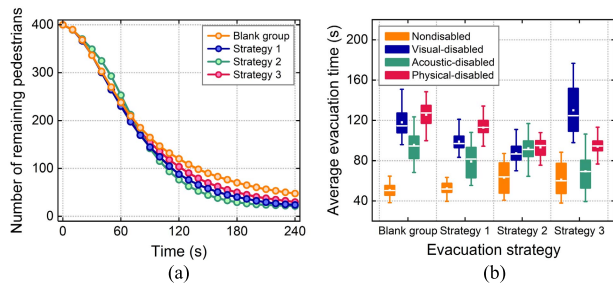


Fig. 12. Analysis of mixed crowd evacuation under different management strategies. (a) Number of remaining pedestrians as a function of time. (b) Box plot of average evacuation time for different types of pedestrians.

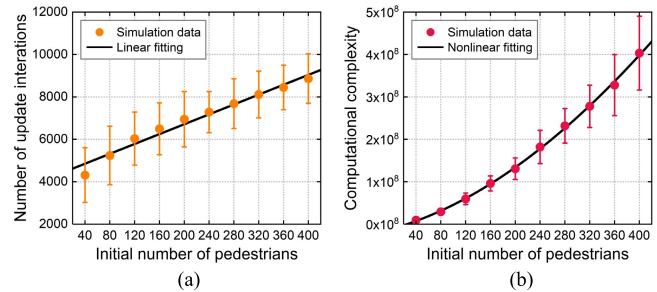


Fig. 14. Computational complexity analysis of this model. (a) Relationship between the number of update iterations and the initial number of pedestrians. (b) Relationship between the computational complexity and the initial number of pedestrians. The data are taken by repeating the simulation 50 times, where the shape point denotes the mean value and the error bar holds the standard deviation.

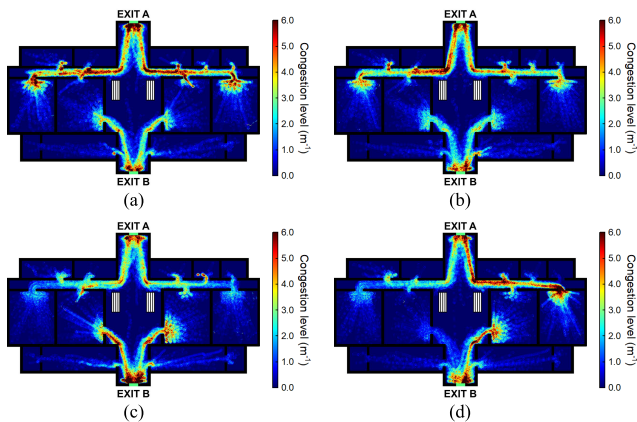


Fig. 13. Spatial characterization of “congestion level” under different management strategies. (a) Blank group. (b) Strategy 1. (c) Strategy 2. (d) Strategy 3.

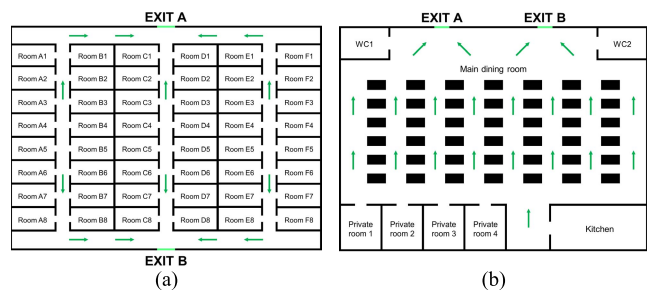


Fig. 15. Schematic diagrams of other simulation scenes. (a) 2-D floor plan of the dormitory scene. (b) 2-D floor plan of the canteen scene.

various guidance facilities for multitype disabled pedestrians are available in each reading room, which also results in

a relatively higher cost. For Strategies 2 and 3, different types of pedestrians are constrained in specific reading areas where targeted guidance facilities are placed, and the costs

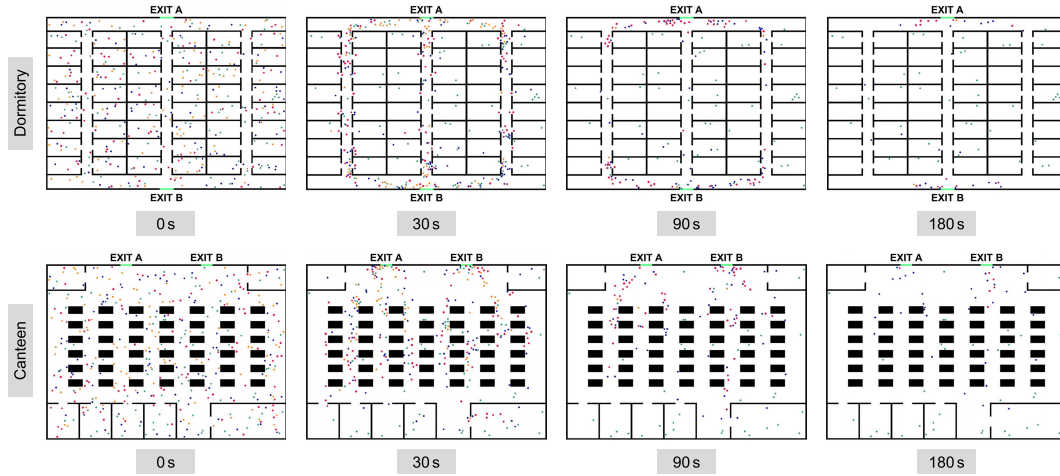


Fig. 16. Snapshots of mixed crowd evacuation in the dormitory and canteen scenes at 0, 30, 90, and 180 s. The orange, blue, green, and pink circles represent nondisabled, visual-disabled, acoustic-disabled, and physical-disabled pedestrians, respectively.

are relatively lower. Notably, the pedestrians with faster speed (nondisabled and acoustic-disabled) are allocated to farther rooms in Strategy 2, while they are assigned to rooms on the same side in Strategy 3. Consequently, targeted assistance in sound, vision, and mobility is supplied to disabled pedestrians by using the guidance facilities, which will alter their responses to emergencies. In this case, the feature parameters are assumed to be transformed as follows:  $\hat{w}_i^{\text{vis}} \rightarrow 0.5w_i^{\text{vis}}$  for visual-disabled pedestrians,  $\hat{w}_i^{\text{aco}} \rightarrow 0.5w_i^{\text{aco}}$  ( $\hat{w}_i^{\text{aco}} = 0$  if  $w_i^{\text{aco}} < 0.1$ ) for acoustic-disabled pedestrians, as well as  $\hat{w}_i^{\text{phy}} \rightarrow 0.5w_i^{\text{phy}}$  for physical-disabled pedestrians.

Fig. 11 displays the snapshots of mixed crowd evacuation in the library scene under different management strategies. The evacuation efficiency of management strategies is significantly higher than that of the blank group, demonstrating that the adoption of guidance facilities is effective. However, the evacuation process differs depending on which management strategy is adopted. As illustrated in Fig. 12(a), the evacuation efficiency of Strategy 1 is slightly faster than that of Strategy 3. The number of remaining pedestrians of Strategy 2 is the largest in the initial stage, but it becomes the least in the subsequent stage. In terms of the average evacuation time, Fig. 12(b) reveals that Strategy 2 is the most effective management strategy in narrowing the gap between disabled and nondisabled pedestrians. The average evacuation time among different types of disabled pedestrians is likewise close in this situation. Moreover, we are interested in the “congestion level” [35] under different management strategies. Compared with the blank group in Fig. 13(a), the various guidance facilities significantly reduce evacuation congestion in Fig. 13(b). Fig. 13(c) and (d) illustrates that Strategy 2 reduces congestion at several bottlenecks on the way to EXIT A but exacerbates it near EXIT B, whereas Strategy 3 relieves congestion on one side but worsens it on the other side. Therefore, the “congestion level” is also an important safety factor to consider when evaluating the management strategy.

As a result, multiple factors such as efficiency, safety, and cost need to be taken into account when determining an effective management strategy. In our case, Strategy 1 can be

adopted if the cost allows because the evacuation efficiency is relatively high and the overall congestion is alleviated. Furthermore, Strategies 2 and 3 have relatively lower costs and allow more disabled pedestrians to escape within a specified time, but whether the exacerbated congestion in certain areas will cause a crowd disaster needs to be considered. In summary, the decision-makers should fully consider the advantages and disadvantages of each management strategy in combination with actual situations to select an appropriate management strategy, which is a critical step to guide the evacuation process and save the lives of vulnerable crowds.

#### E. Model Evaluation and Application Extension

Despite this model having successfully simulated the evacuation process of multitype pedestrians in a library scene, a theoretical analysis of the computational complexity is lacking for model evaluation. Under the assumption that factors with less influence are ignored, the computational complexity of this model is mainly related to the number of pedestrians  $N$  at the initial time. By conducting numerical simulations under different numbers of pedestrians, Fig. 14(a) denotes that the number of update iterations tends to increase linearly with the initial number of pedestrians. From this the computational complexity is defined as the cumulative number of arithmetic operations during each update iteration [36], as shown in Fig. 14(b), the computational complexity is approximately expressed as  $\mathcal{O}(N^3)$  on the basis of the fitting curve. Hence, it should be emphasized that although the computational burden of force-based models is relatively high for large-scale crowds [16], this model is still acceptable to be applied in realistic scenes because it is rare that thousands of disabled pedestrians gather in public places.

Furthermore, several potential scenes are also employed to illustrate the application extension of this model. The disabled community, as one of the gathering places, is able to promote the equal and full integration of the disabled into social life. Here, two of the most common buildings (dormitory and canteen) in disabled communities are selected, as shown in Fig. 15, the dormitory (86.8 m  $\times$  62.6 m) contains 48 rooms

and is equipped with two opposite exits with 5-m width, and the canteen (82.2 m × 59.8 m) contains the main dining room, a kitchen, four private rooms, two WCs, and has two parallel exits with 4-m width. These two scenes generally exist various disabled people and partial nondisabled staff, which satisfies the condition of multitype pedestrians. Under the circumstances, the proposed model is applied to these two scenes, and the snapshots of mixed crowd evacuation are displayed in Fig. 16. It is apparent that similar results are also reflected in different complex environments, which demonstrates that our model is beneficial for implementing the evacuation process of multitype pedestrians.

#### IV. CONCLUSION

In this article, an extended model is proposed to simulate the evacuation process involving multitype disabled pedestrians. To describe the escape movement of disabled pedestrians, the feature parameters that reflect the responses to emergencies are incorporated into the BHSFM. By performing numerical simulations in a library scene, the main conclusions are summarized as follows.

- 1) This model successfully reproduces a more realistic mixed crowd evacuation in the library scene, as well as the motion characteristics of disabled pedestrians.
- 2) The evacuation process is more difficult for disabled pedestrians, in which the remaining number of acoustic-disabled pedestrians is large, and the evacuation efficiency of visual-disabled and physical-disabled pedestrians is slow.
- 3) Three management strategies are proposed to promote the evacuation process, and the appropriate strategy can be determined by considering multiple factors such as efficiency, safety, and cost.

Although this model adequately simulates the evacuation characteristics of disabled pedestrians, its limitations must also be mentioned. First, this model, for the sake of simplicity, ignores the mutual assistance among pedestrians, which is possible to appear during the evacuation process [37]. Second, disabled pedestrians are likely to include more complex types such as deaf-mutes and intellectual impairments, but they are hard to be fully considered in this model. Nonetheless, our model is still a valid attempt to describe the escape movement of multitype pedestrians and provides effective guidance for mixed crowd evacuation. Other management methods, such as offering more effective information to disabled pedestrians [38], establishing specialized escape exits for weak crowds [39], and assigning volunteers to assist with the evacuation process [40], whose effects can also be tested using the proposed model. In general, this work has important values for understanding human collective motion from the perspective of vulnerable crowds.

#### REFERENCES

- [1] M. Moussaïd, D. Helbing, and G. Theraulaz, "How simple rules determine pedestrian behavior and crowd disasters," *Proc. Nat. Acad. Sci. USA*, vol. 108, no. 17, pp. 6884–6888, Apr. 2011.
- [2] H. Alnabulsi and J. Drury, "Social identification moderates the effect of crowd density on safety at the Hajj," *Proc. Nat. Acad. Sci. USA*, vol. 111, no. 25, pp. 9091–9096, Jun. 2014.
- [3] D. Helbing and P. Mukerji, "Crowd disasters as systemic failures: Analysis of the love parade disaster," *EPJ Data Sci.*, vol. 1, no. 1, pp. 1–40, Jun. 2012.
- [4] M. Zhou, H. Dong, B. Ning, and F. Wang, "Recent development in pedestrian and evacuation dynamics: Bibliographic analyses, collaboration patterns, and future directions," *IEEE Trans. Computat. Social Syst.*, vol. 5, no. 4, pp. 1034–1048, Dec. 2018.
- [5] C. S. Jiang, S. Z. Zheng, F. Yuan, H. J. Jia, Z. N. Zhan, and J. J. Wang, "Experimental assessment on the moving capabilities of mobility-impaired disabled," *Saf. Sci.*, vol. 50, no. 4, pp. 974–985, Apr. 2012.
- [6] E. Kuligowski, R. Peacock, E. Wiess, and B. Hoskins, "Stair evacuation of older adults and people with mobility impairments," *Fire Saf. J.*, vol. 62, pp. 230–237, Nov. 2013.
- [7] K. Butler, E. Kuligowski, S. Furman, and R. Peacock, "Perspectives of occupants with mobility impairments on evacuation methods for use during fire emergencies," *Fire Saf. J.*, vol. 91, pp. 955–963, Jul. 2017.
- [8] M. S. Sharifi, K. Christensen, A. Chen, D. Stuart, Y. S. Kim, and Y. Chen, "A large-scale controlled experiment on pedestrian walking behavior involving individuals with disabilities," *Travel Behav. Soc.*, vol. 8, pp. 14–25, Jul. 2017.
- [9] K. Zydek, M. Król, and A. Król, "Evacuation simulation focusing on modeling of disabled people movement," *Sustainability*, vol. 13, no. 4, p. 2405, Feb. 2021.
- [10] X. Zheng, T. Zhong, and M. Liu, "Modeling crowd evacuation of a building based on seven methodological approaches," *Building Environ.*, vol. 44, no. 3, pp. 437–445, Mar. 2009.
- [11] R. L. Hughes, "The flow of human crowds," *Annu. Rev. Fluid Mech.*, vol. 35, no. 1, pp. 169–182, Jan. 2003.
- [12] C. Burstedde, K. Klauck, A. Schadschneider, and J. Zittartz, "Simulation of pedestrian dynamics using a two-dimensional cellular automaton," *Phys. A, Stat. Mech. Appl.*, vol. 295, pp. 507–525, Jun. 2001.
- [13] E. Bonabeau, "Agent-based modeling: Methods and techniques for simulating human systems," *Proc. Nat. Acad. Sci. USA*, vol. 99, no. 3, pp. 7280–7287, May 2002.
- [14] D. Helbing and P. Molnar, "Social force model for pedestrian dynamics," *Phys. Rev. E, Stat. Phys. Plasmas Fluids Relat. Interdiscip. Top.*, vol. 51, no. 5, pp. 4282–4286, May 1995.
- [15] D. Helbing, I. Farkas, and T. Vicsek, "Simulating dynamical features of escape panic," *Nature*, vol. 407, no. 6803, pp. 487–490, Sep. 2000.
- [16] D. C. Duives, W. Daamen, and S. P. Hoogendoorn, "State-of-the-art crowd motion simulation models," *Transp. Res. C, Emerg. Technol.*, vol. 37, pp. 193–209, Dec. 2013.
- [17] J. Kim, C. Ahn, and S. Lee, "Modeling handicapped pedestrians considering physical characteristics using cellular automaton," *Phys. A, Stat. Mech. Appl.*, vol. 510, pp. 507–517, Nov. 2018.
- [18] K. Christensen and Y. Sasaki, "Agent-based emergency evacuation simulation with individuals with disabilities in the population," *J. Artif. Soc. Social Simul.*, vol. 11, no. 3, p. 9, 2008. [Online]. Available: <https://www.jasss.org/11/3/9.html>
- [19] J. Koo, Y. S. Kim, and B.-I. Kim, "Estimating the impact of residents with disabilities on the evacuation in a high-rise building: A simulation study," *Simul. Model. Pract. Theory*, vol. 24, pp. 71–83, May 2012.
- [20] J. Koo, Y. S. Kim, B.-I. Kim, and K. M. Christensen, "A comparative study of evacuation strategies for people with disabilities in high-rise building evacuation," *Expert Syst. Appl.*, vol. 40, no. 2, pp. 408–417, Feb. 2013.
- [21] D. S. Stuart, M. S. Sharifi, K. M. Christensen, A. Chen, Y. S. Kim, and Y. Chen, "Crowds involving individuals with disabilities: Modeling heterogeneity using fractional order potential fields and the social force model," *Phys. A, Stat. Mech. Appl.*, vol. 514, pp. 244–258, Jan. 2019.
- [22] W. Wu, M. Chen, J. Li, B. Liu, and X. Zheng, "An extended social force model via pedestrian heterogeneity affecting the self-driven force," *IEEE Trans. Intell. Transp. Syst.*, vol. 23, no. 7, pp. 1–13, Jul. 2021.
- [23] W. Wu, J. Li, W. Yi, and X. Zheng, "Modeling crowd evacuation via behavioral heterogeneity-based social force model," *IEEE Trans. Intell. Transp. Syst.*, early access, Jan. 25, 2022, doi: [10.1109/TITS.2022.3140823](https://doi.org/10.1109/TITS.2022.3140823).
- [24] J. Drury and S. Reicher, "Collective action and psychological change: The emergence of new social identities," *Brit. J. Social Psychol.*, vol. 39, no. 4, pp. 579–604, Dec. 2000.
- [25] J. Fang, S. El-Tawil, and B. Aguirre, "Leader-follower model for agent based simulation of social collective behavior during egress," *Saf. Sci.*, vol. 83, pp. 40–47, Mar. 2016.



- [26] D. Helbing, M. Isobe, T. Nagatani, and K. Takimoto, "Lattice gas simulation of experimentally studied evacuation dynamics," *Phys. Rev. E, Stat. Phys. Plasmas Fluids Relat. Interdiscip. Top.*, vol. 67, no. 6, Jun. 2003, Art. no. 067101.
- [27] S. P. Hoogendoorn and P. H. Bovy, "Normative pedestrian behaviour theory and modelling," in *Transportation and Traffic Theory in the 21st Century*. Bingley, U.K.: Emerald Group Publishing Limited, Jun. 2002, pp. 219–245.
- [28] G. Fragkos, P. Apostolopoulos, and E. Tsiropoulou, "ESCAPE: Evacuation strategy through clustering and autonomous operation in public safety systems," *Future Internet*, vol. 11, no. 1, p. 20, Jan. 2019.
- [29] M. D'Orazio, E. Quagliarini, G. Bernardini, and L. Spalazzi, "EPES—Earthquake pedestrians' evacuation simulator: A tool for predicting earthquake pedestrians' evacuation in urban outdoor scenarios," *Int. J. Disaster Risk Reduction*, vol. 10, pp. 153–177, Dec. 2014.
- [30] X. Chen, M. Treiber, V. Kanagaraj, and H. Li, "Social force models for pedestrian traffic—State of the art," *Transp. Rev.*, vol. 38, no. 5, pp. 625–653, Nov. 2017.
- [31] E. K. Hwang, "A study on the system improvement for ensuring evacuation safety of people vulnerable to disasters in case of a fire in the building," *Adv. Mater. Res.*, vols. 1065–1069, pp. 2372–2376, Dec. 2014.
- [32] H. Hill, "Disability and accessibility in the library and information science literature: A content analysis," *Library Inf. Sci. Res.*, vol. 35, no. 2, pp. 137–142, Apr. 2013.
- [33] F. K. Cylke, M. M. Moodie, and R. E. Fistick, "Serving the blind and physically handicapped in the United States of America," *Library Trends*, vol. 55, no. 4, pp. 796–808, 2007.
- [34] D. Helbing, L. Buzna, A. Johansson, and T. Werner, "Self-organized pedestrian crowd dynamics: Experiments, simulations, and design solutions," *Transp. Sci.*, vol. 39, no. 1, pp. 1–24, Feb. 2005.
- [35] C. Feliciani and K. Nishinari, "Measurement of congestion and intrinsic risk in pedestrian crowds," *Transp. Res. C, Emerg. Technol.*, vol. 91, pp. 124–155, Jun. 2018.
- [36] S. Boyd, S. P. Boyd, and L. Vandenberghe, *Convex Optimization*. Cambridge, U.K.: Cambridge Univ. Press, 2004.
- [37] T. J. Shields, K. E. Boyce, and N. McConnell, "The behaviour and evacuation experiences of WTC 9/11 evacuees with self-designated mobility impairments," *Fire Saf. J.*, vol. 44, no. 6, pp. 881–893, Aug. 2009.
- [38] C. Feliciani, H. Murakami, K. Shimura, and K. Nishinari, "Efficiently informing crowds—Experiments and simulations on route choice and decision making in pedestrian crowds with wheelchair users," *Transp. Res. C, Emerg. Technol.*, vol. 114, pp. 484–503, May 2020.
- [39] Q. Liu, "The effect of dedicated exit on the evacuation of heterogeneous pedestrians," *Phys. A, Stat. Mech. Appl.*, vol. 506, pp. 305–323, Sep. 2018.
- [40] K. Arai, T. Xuan, and N. Thi, "Task allocation model for rescue disabled persons in disaster area with help of volunteers," *Int. J. Adv. Comput. Sci. Appl.*, vol. 3, no. 7, pp. 1–6, 2012.



**Wenhan Wu** received the B.S. degree from the School of Automation, Central South University, Changsha, China, in 2019. He is currently pursuing the Ph.D. degree in control science and engineering with Tsinghua University, Beijing, China.

His current research interests include collective behavior, emergency evacuation, and pedestrian group dynamics.



**Wenfeng Yi** received the B.S. degree from the School of Astronautics, Beihang University, Beijing, China, in 2019. He is currently pursuing the Ph.D. degree in control science and engineering with Tsinghua University, Beijing.

His current research interests include collective behavior, emergency evacuation, and pedestrian queueing dynamics.



**Jinghai Li** received the B.S. degree in automation and the M.S. degree in control science and engineering from Tianjin University, Tianjin, China, in 2009 and 2016, respectively, and the Ph.D. degree in control science and engineering from Tsinghua University, Beijing, China, in 2022.

He is currently a Post-Doctoral Researcher with the School of Mechanical and Electrical Engineering, Beijing University of Chemical Technology, Beijing. His current research interests include crowd dynamics, control of robotic systems, and adaptive systems.

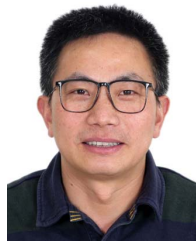


**Maoyin Chen** (Member, IEEE) received the B.S. degree in mathematics and the M.S. degree in control theory and control engineering from Qufu Normal University, Qufu, Shandong, China, in 1997 and 2000, respectively, and the Ph.D. degree in control theory and control engineering from Shanghai Jiao Tong University, Shanghai, China, in 2003.

From 2003 to 2005, he was a Post-Doctoral Researcher with the Department of Automation, Tsinghua University, Beijing, China, where he has been an Associate Professor since October 2008.

From 2006 to 2008, he visited Potsdam University, Potsdam, Germany, as an Alexander von Humboldt Research Fellow. He has authored or coauthored more than 100 peer-reviewed international journal articles. His research interests include fault prognosis and complex systems.

Dr. Chen has won the First Prize in natural science (2011, ranked first) and the Second Prize (2019, ranked first) of Chinese Association of Automation (CAA).



**Xiaoping Zheng** received the B.S. degree from the Chengdu University of Traditional Chinese Medicine (TCM), Chengdu, China, in 1995, and the Ph.D. degree from Sichuan University, Chengdu, in 2003.

From 2004 to 2006, he was a Post-Doctoral Researcher with the School of Management, Fudan University, Shanghai, China. From 2006 to 2013, he was a Professor with the Institute of Safety Management, Beijing University of Chemical Technology, Beijing, China. He is currently a Professor with the Department of Automation, Tsinghua University,

Beijing. His current research interests include large-scale crowd evacuation, evolutionary game theory, and terahertz technology.

Prof. Zheng was the 973 Chief Scientist in 2011 and a recipient of the National Science Fund for Distinguished Young Scholars in 2012.